Learning Robust, Agile, Natural Legged Locomotion Skills in the Wild

Yikai Wang*
Weiyang College
Tsinghua University
China
wangyiji20@mails.tsinghua.edu.cn

Zheyuan Jiang*
Institute for Interdisciplinary Information Sciences
Tsinghua University
China
zy-jiang21@mails.tsinghua.edu.cn

Jianyu Chen†
Institute for Interdisciplinary Information Sciences
Tsinghua University
China
jianyuchen@mail.tsinghua.edu.cn

Abstract: Recently, reinforcement learning has become a promising and polular solution for robot legged locomotion. Compared to model-based control, reinforcement learning based controllers can achieve better robustness against uncertainties of environments through sim-to-real learning. However, the corresponding learned gaits are in general overly conservative and unatural. In this paper, we propose a new framework for learning robust, agile and natural legged locomotion skills over challenging terrain. We incorporate an adversarial training branch based on real animal locomotion data upon a teacher-student training pipeline for robust sim-to-real transfer. Empirical results on both simulation and real world of a quadruped robot demonstrate that our proposed algorithm enables robustly traversing challenging terrains such as stairs, rocky ground and slippery floor with only proprioceptive perception. Meanwhile, the gaits are more agile, natural, and energy efficient compared to the baselines. Both qualitative and quantitative results are presented in this paper. Videos in the supplementary material.

Keywords: Legged Locomotion, Reinforcement Learning, Adversarial Training, Sim to Real

1 Introduction

Locomotion controller design for legged robots has been an important research topic in robotics. For decades, researchers have developed successful model-based control approaches to control legged robots [1, 2, 3]. However, these controllers generally involve extensive human engineering, and are difficult dealing with complex environments such as challenging terrains. Recently, reinforcement learning becomes an increasingly popular control approach for legged robots. A general paradigm involves training control policies in simulation to optimize expected cumulative rewards, followed by transferring these policies to real robots [4]. In comparison to traditional model-based control approaches, reinforcement learning reduces the need for extensive human engineering and has shown more impressive results, including traversing challenging terrains [5, 6], recovering from unhealthy states [7], and navigating complex environments [8].

*Equal contribution.
†Jianyu Chen is also with Shanghai Qizhi Institute, China.

While sim-to-real reinforcement learning exhibits robust legged locomotion skills with appealing properties, in practice, directly optimizing a task reward can lead to policies that produce behaviors undesirable to be applied in real robots, such as unnatural gaits, large contact forces, and high energy consumption. To address these challenges, previous studies have primarily employed intricate reward functions that penalize undesirable behaviors while promoting specific gait patterns[4]. Nevertheless, the process of reward engineering is laborious, and the resulting gaits still frequently appear unnatural.

To address the challenges posed by reward engineering and to achieve more natural gaits, adversarial motion priors (AMP) [9] a promising approach which leverages motion capture data and utilizes adversarial imitation learning to acquire locomotion tasks that closely resemble real-world motion data. While such method has demonstrated successful transfer from simulation to a real quadrupedal robot [10], the learned control policy is limited to traversing flat terrain in a laboratory environment, thereby lacking the capability to handle challenging terrains such as stairs or slippery ground. An intuitive extension is to train the control policy in simulation environments that incorporate different types of terrain. However, based on our experiment results, policies trained with this approach fail to achieve satisfied rewards even within simulation.

In this paper, we propose a new framework which enables learning not only robust, but also agile and natural legged locomotion skills over challenging terrains in the wild. We adopt a teacher-student training paradigm to enable adaptation in real world, where the teacher policy is trained with encoded privileged information, and the student policy is trained to infer the information from historical observations. Several techniques are applied to enhance the robustness of the policy. We then incorporate an adversarial training branch into this teacher-student training pipeline to match the learned skills with real animal motion capture data. We evaluate our method on a quadruped robot in both simulation and real world. Experiment results show that our method successfully learn legged locomotion skills to traverse challenging terrains such as stairs, rocky ground and slippery floor. Meanwhile, compared to baselines, the learned gaits are more agile, natural, and energy efficient. We also find the policy is able to smoothly transit different gaits for different velocity command and terrains.

2 Related Work

2.1 Reinforcement Learning for Legged Locomotion

Recent advancements in deep reinforcement learning for legged locomotion have demonstrated its promising future. Lee et al. [5] applied teacher-student training to the quadruped robot ANYmal, resulting in a robust controller capable of traversing challenging terrains. Peng et al. [11] introduced the use of Deep Mimic [12] to learn robotic locomotion skills by imitating animals. Kumar et al. [6] trained locomotion policies with rapid motor adaptation, enabling them to quickly adapt to environmental changes. Building upon this, Kumar et al. [13] extended the RMA algorithm to the bipedal robot Cassie. Yang et al. [8] employed a cross-modal transformer to learn an end-to-end controller for quadrupedal navigation in complex environments. Ji et al. [14] trained a neural network state estimator to estimate robot states that cannot be directly inferred from sensory data. Escontrela et al. [10] utilized Adversarial Motion Priors (AMP) to train control policies for a quadrupedal robot, highlighting that AMP can effectively substitute complex reward functions. Sharma et al. [15] trained a reinforcement learning controller using unsupervised skill discovery and successfully transferred it to a real quadruped robot. Xie et al. [16] revisited the necessity of dynamics randomization in legged locomotion and provided suggestions on when and how to employ dynamics randomization. Bohez et al. [17] trained a low-level locomotion controller for a quadruped robot by imitating real animal data, utilizing this controller to accomplish various tasks. Margolis et al. [18] trained policies to perform jumps from pixel inputs, while Miki et al. [19] trained a locomotion controller using observations of the height map of the terrain around the robot's base. Rudin et al. [4] employed massively parallel simulation environments to significantly accelerate the training process of a locomotion controller. Margolis et al. [20] trained a locomotion controller

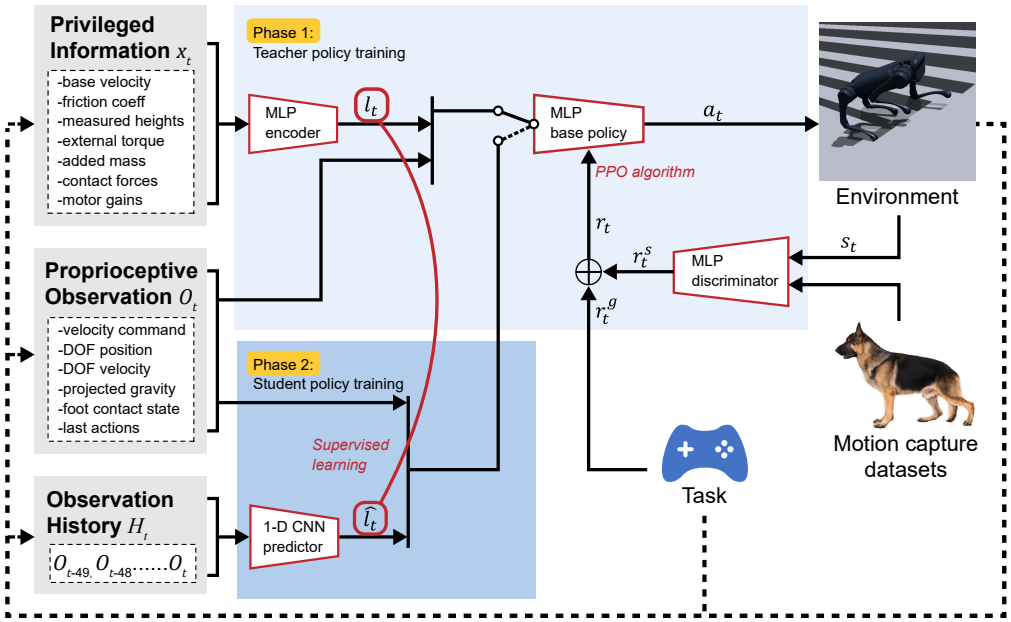

Figure 1: Overview of methods: The teacher policy comprises an encoder (MLP) responsible for encoding privileged information into an 8-dimensional latent vector l, and a base policy (MLP) that generates PD targets. The base policy is conditioned on both l and the proprioceptive observation. The training process is divided into two phases, utilizing the 'teacher-student' framework. In the first phase, the base policy and encoder are jointly trained, while the discriminator is simultaneously trained using a motion capture dataset to provide a style reward for policy training. In the second phase, the predictor is trained through supervised learning to replace the teacher encoder and predict the latent representation from historical observations.

for the Mini Cheetah robot, enabling it to achieve speeds of up to 3.9m/s, surpassing traditional controllers' speeds by a large margin. Other notable works include directly learning locomotion skills in the real world [21, 22], as well as learning locomotion skills for bipedal robots [23, 24, 25].

2.2 Motion Control from Real World Motion Data

Imitating a reference motion dataset offers an approach to designing controllers for skills that are challenging to manually encode. Pollard et al. [26, 27, 28, 29] employ motion tracking techniques, where characters explicitly mimic the sequence of poses from reference trajectories. Learning from real-world motion provides an alternative to crafting complex rewards for synthesizing natural motion. Peng et al. [12] adapt reinforcement learning (RL) methods to learn robust control policies capable of imitating a wide range of example motion clips. Leveraging GAN-style training, Peng et al. [9] learn a "style" reward from a reference motion dataset to control the character's low-level movements, while allowing users to specify high-level task objectives. Escontrela et al. [10] utilize the framework proposed by Peng et al. [9] to train a locomotion policy for a quadrupedal robot to traverse flat ground. Additionally, Peng et al. [30] present a scalable adversarial imitation learning framework that enables physically simulated characters to acquire a wide repertoire of motor skills, which can be subsequently utilized to perform various downstream tasks.

3 Method

The proposed approach comprises several building blocks which mainly support robust sim-to-real learning as well as natural gait learning from motion capture reference. An overview of the proposed framework is shown in Figure 1. We first have a phase 1 training process, which learns a teacher policy using both proprioceptive observation and the privileged information. An adversarial training process is running simultaneously to enforce agile and natural gait from motion capture reference data. Then at the phase 2 training process, we learn a student policy which takes the historical proprioceptive observations and output the final actions with the policy. This policy are directly deployed to the real robot which bridges the sim-to-real gap. In this section, we will introduce the details of each component.

3.1 Robust Sim-to-Real Locomotion Learning

To enable robust legged locomotion through sim-to-real learning, we adopt a teacher-student training framework, augmented with several tricks to enhance sim-to-real transfer.

3.1.1 Teacher-Student Training Framework

Inspired by previous works for robust legged locomotion learning [5, 6], we integrate the teacher-student training paradigm into our framework. The teacher policy encodes privileged information of the environments and the robot from the simulation, while the student policy only takes observations directly available from sensors on the real robot. Thus, the privileged simulation information enables good performance for the teacher policy in challenging environments, which is then adopted to teach the student policy to perform equally well in the real world.

Teacher Policy Training: We can formulate the teacher policy training problem as a Markov Decision Process (MDP) [31]. An MDP can be represented by a tuple $(\mathcal{S}, \mathcal{A}, \mathcal{P}, R, \gamma)$, where $\mathcal{S}$ and $\mathcal{A}$ denote the state and action spaces, respectively. The transition probability function $\mathcal{P} : \mathcal{S} \times \mathcal{A} \times \mathcal{S} \rightarrow [0, 1]$ maps the current state and action to the probability distribution of the next state, based on the robot and environment dynamics. The reward function $R : \mathcal{S} \times \mathcal{A} \rightarrow \mathbb{R}$ assigns a real value to each state-action pair. The discount factor γ determines the importance of future rewards. The goal of reinforcement learning is to find a policy $\pi : \mathcal{S} \rightarrow \mathcal{A}$ to maximize the the expected future cumulative rewards $J_R(\pi) = \mathbb{E}_{\tau\sim\pi}\left[\sum_{t=0}^{\infty} \gamma^t R(s_t, a_t)\right]$.

In our work, the state s is composed of both the proprioceptive observation O_t and a latent vector l_t. Here l_t contains encoded privileged information using an encoder $l_t = \mu(x_t)$. Then a base policy π maps the concatenated state $s_t = (l_t, O_t)$ to the action command a_t. Compared to previous works, we incorporate additional data in the privileged information, such as the robot base velocity and measured terrain heights represented as 3D points. By learning the encoder along with the reinforcement learning process, the encoded latent l_t is expected to contain rich information about the robot dynamics, state estimation, and environment factors. Detailed definition about the privileged information, the proprioceptive observation, as well as the action space can be found in Appendix A.1. We choose proximal policy optimization (PPO) as our backbone reinforcement learning algorithm. Detailed design of the network architectures and algorithm hyper-parameters can be found in Appendix A.2 and A.3.

Student Policy Training: The teacher policy cannot be directly deployed to the real robot, since the privileged information is generally only available in simulation, but non-trivial or impractical to obtain in real world. Therefore, after training the teacher policy, we train a student policy which mimic the functionalities of the teacher policy, but is feasible to be directly deployed on the real robot. To do this, we train a different encoder $\hat{\mu}$, which takes a series of historical proprioceptive observations $O_{t-T}, ..., O_{t-1}, O_t$ as inputs, instead of the privileged information. Such historical observations are easily obtained on real robot by creating memory buffer for sensor inputs. This encoder is then trained using supervised learning to minimize the error between the encoder output $\hat{l}_t$ and the ground truth latent l_t: $||\hat{l}_t - l_t||^2$. The intuition underneath is that, according to the gen-

eral assumption of partially observable Markov decision process (POMDP) [32], the unobservable true state such as the privileged information can be recovered from historical observations. After obtaining the latent $\hat{l}_t$, we use the same base policy π with the teacher policy to compute the action a_t, which is then directly applied to the real robot actuators. Detailed implementation of this part can be found in Appendix A.1 and A.2.

3.1.2 Enhancing Sim-to-Real Transfer

Upon the teacher-student training paradigm, we also incorporate several important techniques to enhance the sim-to-real transfer performance, including domain randomization, terrain curriculum, and action filtering.

Domain Randomization: Domain randomization is the most important practical techniques for robot sim-to-real transfer. In general, the sim-to-real problem mainly lies on the gap between the dynamics models of simulation and real world, as well as the the gap between their state distributions. In essence, if we randomize both the dynamics and the state distribution in the simulation, so that the randomization range covers the real world setting, then learned policy should be robust in real world environments. We randomize both robot dynamics, such as mass and motor gain, as well as environment dynamics, such as friction coefficient. Besides randomizing dynamics, we also add perturbations to the robot on its linear velocity, angular velocity, as well as actuator torques. Furthermore, we add noises to sensor observations. Please refer to Appendix A.5 for detailed ranges of the randomization and perturbation we apply.

Terrain Curriculum: Besides the above randomization terms, we generate random terrains in simulation during training, in order to generalize to various ground environment in the real world. We adopt the game-inspired terrain curriculum proposed in [4]. Specifically, we utilize four types of terrains: plane ground, uniform noise, discrete obstacles, and stairs. Before proceeding to a more challenging type of terrain, the robot needs to successfully traverse the current terrain and achieve a satisfied task reward. In each type of terrain, we also increase the difficulty for later episodes. This adaptive curriculum mechanism enables us to stably learn robust locomotion skills for the robot.

Action Filtering: We observed that applying a low-pass filter to the output actions can significantly improve the smoothness of motions, enabling better sim-to-real transfer. The filter is defined as:

$$u_t = 0.2 * u_{t-1} + 0.8 * a_t$$

where u_t represents the filtered target joint angles applied to the low-level PD controllers, and a_t corresponds to the action output by the neural network policy.

3.2 Natural Gait Learning with Motion Capture Reference

We hope the learned locomotion skills to be not only robust, but also natural and agile just like real animals. Inspired by adversarial motion priors (AMP) [9], we incorporate an adversarial motion style matching process into our framework, in order to learn robust, agile, and natural legged locomotion skills.

Adversarial Motion Style Matching: In order to learn agile and natural gaits, our designed reward for the reinforcement learning problem consists of both a "task" reward r_t^g and a "style" reward r_t^s. The overall reward function is given by $r_t = \omega^g r_t^g + \omega^s r_t^s$. The task reward is defined based on the specific task we aim to accomplish, here it consists of a linear velocity command tracking reward and an angular velocity command tracking reward:

$$r_t^g = w^v \exp\left(-|\hat{v}_t^{\text{xy}} - v_t^{\text{xy}}|\right) + w^\omega \exp\left(-|\hat{\omega}_t^z - \omega_t^z|\right) \tag{1}$$

where w^v, w^ω, and w^τ are the coefficients. $\hat{\hat{v}}_t^{\text{xy}}$ and $\hat{\omega}_t^z$ represent the linear and angular velocity commands, respectively. To ensure robustness and learn diverse gait patterns, different ranges of velocity commands are defined for each terrain type, as listed in Appendix A.4. The velocity commands are randomly sampled from the specified ranges.

The style reward is generated by a discriminator $r_t^s = \phi(s_t, s_{t+1})$, which is trained to classify whether the given state transition samples are from the motion capture dataset or from the policy rollouts. The optimization objective of the discriminator is as follows:

$$\begin{aligned}\arg\min_{\phi} \mathbb{E}_{(s,s')\sim\mathcal{D}}\left[\left(D_\phi\left(s,s'\right)-1\right)^2\right] \\ + \mathbb{E}_{(s,s')\sim\pi_\theta(s,a)}\left[\left(D_\phi\left(s,s'\right)+1\right)^2\right] \\ + \frac{w^{\text{gp}}}{2}\mathbb{E}_{(s,s')\sim\mathcal{D}}\left[\left\|\nabla_\phi D_\phi\left(s,s'\right)\right\|^2\right],\end{aligned} \tag{2}$$

where $\mathcal{D}$ denotes the motion capture dataset, and ω^{gp} is the coefficient for gradient penalty which reduces oscillations in the adversarial training process. The style reward is then defined as:

$$r_t^s(s_t, s_{t+1}) = \max\left\{0, 1 - 0.25(\phi(s_t, s_{t+1}) - 1)^2\right\} \tag{3}$$

Therefore, the policy is trained through reinforcement learning to maximize the reward function as a generator, while the discriminator is trained using both the motion dataset $\mathcal{D}$ and the data generated during policy rollouts, forming an adversarial motion style matching framework.

Motion Capture Data Reference: We utilize high-quality dog motion capture data provided by Zhang et al. [33]. The dataset was obtained from a real German shepherd, which exhibits different morphology compared to our quadrupedal robot. To adapt the dog motion data to our robot, we apply inverse kinematics for motion retargeting as employed in Peng et al. [11]. Furthermore, we enhance the motion capture data by mirroring the dataset, specifically by switching the joint angle sequences between the left and right legs and reflecting the base position of the robot. Empirically, we find that this enhancement results in more symmetrical and natural-looking gaits.

4 Experiments

We use Isaac Gym [34] simulator for training. The learned policy is then deployed to real robot. We use Unitree A1 as our robot platform in both simulation and real world, which is a medium-sized quadrupedal robot. The robot's motor encoders provide joint angles and angular velocities, the IMU provides projected gravity information, and the foot force sensors obtain binary contact states. we compare the performance of our approach with two baselines:

- **Complex rewards**: Policy trained with typical model-free RL method using complex hand-designed reward function as in [4].
- **AMP**: Policy trained using adversarial motion priors as style reward to learn agile and natural legged locomotion skills [10].

We conduct both simulation and real world experiments to evaluate out method, which demonstrate that our method outperforms baselines by learning robust, agile, natural and energy-efficient legged locomotion skills.

4.1 Simulation Experiments

Metrics: In simulation experiments, we compare the performance of our approach with the comparison baselines on following metrics:

- **Success rate**: Success means no falling before reaching the goal position in less than a threshold time. The success rate is calculated as the ratio of successful trials to the total number of experiments conducted.
- **TTF**: The time to fall normalized by the maximum duration of trajectories.
- **Command tracking accuracy**: The average velocity command tracking reward as defined in Equation (1).

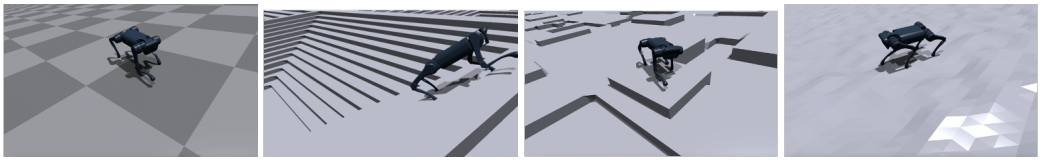

Figure 2: Simulation experiments.

- **Energy efficiency**: The energy efficiency is estimated by computing the average power of motors, which is defined as: $\sum_{\text{motors}}[\tau\dot{\theta}]^+$, where τ is the joint torque, and $\dot{\theta}$ is the motor velocity.

Note that we only measure energy efficiency and command tracking accuracy of a policy when its success rate exceeds 60%.

Terrains: We evaluate the learned policies on three kinds of challenging terrains:

- **Stairs**: Continuous stairs in surroundings with step height of 14cm and step width of 31cm.
- **Discrete obstacles**: Randomly place discrete obstacles on the ground with height of 15cm, or pit with depth of 15cm.
- **uniform noise**: Uneven ground generated by adding uniform noise to the terrain heights.

Examples of different terrains in simulation are show in Figure 2.

Results: Results of the evaluation metrics in simulations are shown in tables in Appendix B.1. Each data in the chart was an average over 1000 experiments. We can see that our controller can successfully traverse through a greater variety of complex terrains with higher success rate, this might be due to the diverse motion capture data that enables the robot to switch to the most suitable gait or blend different gaits at different terrains and speeds. Meanwhile, the teacher-student training architecture plays an important role in state estimation and system identification.

Furthermore, our controller performs better in terms of energy efficiency and command tracking accuracy under different terrains and speed commands. In details, on relatively simple terrains with uniform noise, the command tracking accuracy of the complex rewards performs well, but its energy efficiency increases rapidly with increasing speed. The energy efficiency of AMP remains low, but this is because it cannot track the high velocity commands well. It is worth mentioning that although the energy efficiency of complex rewards is relatively good at low speeds, it is significantly worse than that in our real world experiments, which demonstrates the advantage of our methods in terms of sim-to-real transfer. One interesting observation is that the learned controller can smoothly transit to different gait in order to respond to different velocity commands and different terrains, as shown in Figure 4 of Appendix B.1.

4.2 Real World Experiments

Metrics: In real world experiments, we compare the performance of our approach with the comparison baselines on following metrics:

- **TTF**: Time to fall normalized by a threshold time. If robot does not fall during the threshold time, TTF is 1.
- **Success rate**: The definition is same as Section 4.1. To avoid damage to the robot, if the robot falls down in three consecutive experiments, its success rate is set to 0.
- **Distance**: The distance the robot traverses in the threshold time, normalized by the desired distance. If the robot reach the desired distance in within the threshold time, then the distance is set to 1.

Results: We evaluate the performance of controllers on the real robot in different settings as follows. Sample outcomes are shown in Figure 3, videos can be found in the supplementary materials.

Figure 3: Real world experiments.

- **Floating barrier high 13-cm**: We test the robot's capability of climbing over high obstacles placed on slippery ground. Both our controller and the baselines do not leverage any visual information. As for our controller, when the front legs are obstructed, one of the front legs immediately lifts upwards, while the other front leg extends, making the body to tilt upwards. Then the hind legs push with force to climb over the obstacle smoothly. This demonstrates the robot's capability to naturally switch gaits by utilizing past observations.
- **Grassland**: There are many bumps and pits on the grassland. The robot with our controller can quickly adjust its posture to maintain balance when encountering obstacles, and move forward in walking and gallop gaits under different speed commands. As a comparison, the robot with AMP controller could not traverse rough grassland even at low speeds command. The controller trained with complex rewards has better robustness than AMP. But its success rate was lower than ours, and it could only walk at low speeds in a single gait.
- **Extremely slippery ground**: We create an extremely slippery surface by pouring oil onto plastic sheets. When the robot walks from the ground to the plastic sheet, it immediately adapts and switches to a more conservative gait, noticeably reducing its foot lift height, resulting in a gait resembling 'glide' on the slippery surface. As a comparison, the robots with baseline controllers did not alter their gait on smooth surfaces, making it difficult to maintain balance and is easy to fall.
- **Staircase high 8-cm**: Without visual information assistance, out method can successfully climb the stairs. This means our method enables the robot to continuously adjust its posture based on proprioceptive information. Furthermore, compared to previous method, our learned policy can climb the stairs with a pretty agile and natural gait.
- **Slopes**: Although our robot has not been trained on slopes in simulation, it can successfully adapt to a slope of approximately 30 degrees. This demonstrates the good generalization and robustness capabilities of our method.

The quantitative results are shown in Table 6 in Appendix B.2. We can see that our method outperforms all baselines in terms of the success rate, TTF and distance metrics. Note that the real world terrains are even more complex and diverse than that in simulation, with many unknown physical factors. Therefore, conducting real world experiments places high demands on the robustness of the controllers. Furthermore, we found that processing the output actions with a low-pass filter could smooth the motions to improve energy efficiency notably. We conducted ablation studies about the low-pass-filter for energy efficiency. As shown in Table 5 in Appendix B.2, our approach exhibits better energy efficiency while tracking different velocity command, whether with the filter or not.

5 Conclusion

In this paper, we proposed a novel framework which enables learning legged locomotion skills that are robust, agile, natural and energy efficient in real world challenging terrain environments. By

adopting the teacher-student training paradigm, we obtained an encoder to infer environmental factors for adaptation in the real world. Several techniques are applied to enhance the robustness of the learned policy. Through the integration of an adversarial training branch, the learned gait is enforced to match the style of real animal motion capture data. Extensive results of a quadruped robot conducted in both simulation and real world showcased the superior performance of our proposed algorithm compared to baseline approaches.

Despite the advantages of our algorithm, it does possess certain limitations. Our framework incorporates an adversarial training and the reinforcement learning problem involves optimizing the joint rewards, including both task rewards and style rewards. However, such adversarial training is time-consuming and it is currently hard to leverage large scale motion capture dataset. Future research could try to decouple the learning process for style matching and task finishing. For instance, one approach could be pretraining a low-level controller using a large-scale dataset to match the desired style, and subsequently training the controller to handle a wider range of downstream tasks.

References

[1] J. Di Carlo, P. M. Wensing, B. Katz, G. Bledt, and S. Kim. Dynamic locomotion in the mit cheetah 3 through convex model-predictive control. In *2018 IEEE/RSJ international conference on intelligent robots and systems (IROS)*, pages 1–9. IEEE, 2018.

[2] A. W. Winkler, C. D. Bellicoso, M. Hutter, and J. Buchli. Gait and trajectory optimization for legged systems through phase-based end-effector parameterization. *IEEE Robotics and Automation Letters*, 3(3):1560–1567, 2018.

[3] K. Byl and R. Tedrake. Dynamically diverse legged locomotion for rough terrain. In *2009 IEEE International Conference on Robotics and Automation*, pages 1607–1608. IEEE, 2009.

[4] N. Rudin, D. Hoeller, P. Reist, and M. Hutter. Learning to walk in minutes using massively parallel deep reinforcement learning. In *Conference on Robot Learning*, pages 91–100. PMLR, 2022.

[5] J. Lee, J. Hwangbo, L. Wellhausen, V. Koltun, and M. Hutter. Learning quadrupedal locomotion over challenging terrain. *Science robotics*, 5(47):eabc5986, 2020.

[6] A. Kumar, Z. Fu, D. Pathak, and J. Malik. Rma: Rapid motor adaptation for legged robots. *arXiv preprint arXiv:2107.04034*, 2021.

[7] J. Lee, J. Hwangbo, and M. Hutter. Robust recovery controller for a quadrupedal robot using deep reinforcement learning. *arXiv preprint arXiv:1901.07517*, 2019.

[8] R. Yang, M. Zhang, N. Hansen, H. Xu, and X. Wang. Learning vision-guided quadrupedal locomotion end-to-end with cross-modal transformers. *arXiv preprint arXiv:2107.03996*, 2021.

[9] X. B. Peng, Z. Ma, P. Abbeel, S. Levine, and A. Kanazawa. Amp: Adversarial motion priors for stylized physics-based character control. *ACM Transactions on Graphics (TOG)*, 40(4): 1–20, 2021.

[10] A. Escontrela, X. B. Peng, W. Yu, T. Zhang, A. Iscen, K. Goldberg, and P. Abbeel. Adversarial motion priors make good substitutes for complex reward functions. In *2022 IEEE/RSJ International Conference on Intelligent Robots and Systems (IROS)*, pages 25–32. IEEE, 2022.

[11] X. B. Peng, E. Coumans, T. Zhang, T.-W. Lee, J. Tan, and S. Levine. Learning agile robotic locomotion skills by imitating animals. *arXiv preprint arXiv:2004.00784*, 2020.

[12] X. B. Peng, P. Abbeel, S. Levine, and M. Van de Panne. Deepmimic: Example-guided deep reinforcement learning of physics-based character skills. *ACM Transactions On Graphics (TOG)*, 37(4):1–14, 2018.

[13] A. Kumar, Z. Li, J. Zeng, D. Pathak, K. Sreenath, and J. Malik. Adapting rapid motor adaptation for bipedal robots. In *2022 IEEE/RSJ International Conference on Intelligent Robots and Systems (IROS)*, pages 1161–1168. IEEE, 2022.

[14] G. Ji, J. Mun, H. Kim, and J. Hwangbo. Concurrent training of a control policy and a state estimator for dynamic and robust legged locomotion. *IEEE Robotics and Automation Letters*, 7(2):4630–4637, 2022.

[15] A. Sharma, M. Ahn, S. Levine, V. Kumar, K. Hausman, and S. Gu. Emergent real-world robotic skills via unsupervised off-policy reinforcement learning. *arXiv preprint arXiv:2004.12974*, 2020.

[16] Z. Xie, X. Da, M. Van de Panne, B. Babich, and A. Garg. Dynamics randomization revisited: A case study for quadrupedal locomotion. In *2021 IEEE International Conference on Robotics and Automation (ICRA)*, pages 4955–4961. IEEE, 2021.

[17] S. Bohez, S. Tunyasuvunakool, P. Brakel, F. Sadeghi, L. Hasenclever, Y. Tassa, E. Parisotto, J. Humplik, T. Haarnoja, R. Hafner, et al. Imitate and repurpose: Learning reusable robot movement skills from human and animal behaviors. *arXiv preprint arXiv:2203.17138*, 2022.

[18] G. B. Margolis, T. Chen, K. Paigwar, X. Fu, D. Kim, S. Kim, and P. Agrawal. Learning to jump from pixels. *arXiv preprint arXiv:2110.15344*, 2021.

[19] T. Miki, J. Lee, J. Hwangbo, L. Wellhausen, V. Koltun, and M. Hutter. Learning robust perceptive locomotion for quadrupedal robots in the wild. *Science Robotics*, 7(62):eabk2822, 2022.

[20] G. B. Margolis, G. Yang, K. Paigwar, T. Chen, and P. Agrawal. Rapid locomotion via reinforcement learning. *arXiv preprint arXiv:2205.02824*, 2022.

[21] P. Wu, A. Escontrela, D. Hafner, K. Goldberg, and P. Abbeel. Daydreamer: World models for physical robot learning. *arXiv preprint arXiv:2206.14176*, 2022.

[22] L. Smith, I. Kostrikov, and S. Levine. A walk in the park: Learning to walk in 20 minutes with model-free reinforcement learning. *arXiv preprint arXiv:2208.07860*, 2022.

[23] Z. Xie, P. Clary, J. Dao, P. Morais, J. Hurst, and M. van de Panne. Iterative reinforcement learning based design of dynamic locomotion skills for cassie. *arXiv preprint arXiv:1903.09537*, 2019.

[24] J. Siekmann, K. Green, J. Warila, A. Fern, and J. Hurst. Blind bipedal stair traversal via sim-to-real reinforcement learning. *arXiv preprint arXiv:2105.08328*, 2021.

[25] J. Siekmann, Y. Godse, A. Fern, and J. Hurst. Sim-to-real learning of all common bipedal gaits via periodic reward composition. In *2021 IEEE International Conference on Robotics and Automation (ICRA)*, pages 7309–7315. IEEE, 2021.

[26] N. S. Pollard, J. K. Hodgins, M. J. Riley, and C. G. Atkeson. Adapting human motion for the control of a humanoid robot. In *Proceedings 2002 IEEE international conference on robotics and automation (Cat. No. 02CH37292)*, volume 2, pages 1390–1397. IEEE, 2002.

[27] D. B. Grimes, R. Chalodhorn, and R. P. Rao. Dynamic imitation in a humanoid robot through nonparametric probabilistic inference. In *Robotics: science and systems*, pages 199–206. Cambridge, MA, 2006.

[28] W. Suleiman, E. Yoshida, F. Kanehiro, J.-P. Laumond, and A. Monin. On human motion imitation by humanoid robot. In *2008 IEEE International conference on robotics and automation*, pages 2697–2704. IEEE, 2008.

[29] K. Yamane, S. O. Anderson, and J. K. Hodgins. Controlling humanoid robots with human motion data: Experimental validation. In *2010 10th IEEE-RAS International Conference on Humanoid Robots*, pages 504–510. IEEE, 2010.

[30] X. B. Peng, Y. Guo, L. Halper, S. Levine, and S. Fidler. Ase: Large-scale reusable adversarial skill embeddings for physically simulated characters. *ACM Transactions On Graphics (TOG)*, 41(4):1–17, 2022.

[31] M. L. Puterman. Markov decision processes. *Handbooks in operations research and management science*, 2:331–434, 1990.

[32] L. P. Kaelbling, M. L. Littman, and A. R. Cassandra. Planning and acting in partially observable stochastic domains. *Artificial intelligence*, 101(1-2):99–134, 1998.

[33] H. Zhang, S. Starke, T. Komura, and J. Saito. Mode-adaptive neural networks for quadruped motion control. *ACM Transactions on Graphics (TOG)*, 37(4):1–11, 2018.

[34] V. Makoviychuk, L. Wawrzyniak, Y. Guo, M. Lu, K. Storey, M. Macklin, D. Hoeller, N. Rudin, A. Allshire, A. Handa, and G. State. Isaac gym: High performance gpu-based physics simulation for robot learning, 2021.

[35] J. Schulman, F. Wolski, P. Dhariwal, A. Radford, and O. Klimov. Proximal policy optimization algorithms. *CoRR*, abs/1707.06347, 2017. URL http://arxiv.org/abs/1707.06347.

[36] J. Schulman, P. Moritz, S. Levine, M. Jordan, and P. Abbeel. High-dimensional continuous control using generalized advantage estimation. In *Proceedings of the International Conference on Learning Representations (ICLR)*, 2016.

A Implementation Details

A.1 State and Action Spaces

The output action a_t comprises a 12-dim target joint angle vector. The observation o_t is a 46-dim vector containing the 3-dim velocity command, 12-dim joint positions, 12-dim joint velocities, 3-dim projected gravity, 4-dim binary foot-contact states, and 12-dim last actions. The privileged information x_t is a 233-dim vector that includes the linear and angular velocity in the base frame (6-dim), friction coefficient, measured heights of some surrounding points (187-dim), external torque applied to the base (2-dim), stiffness and damping of each motor (24-dim), added mass to the base, and foot contact forces (4-dim). The encoder takes x_t as input, while the predictor takes the history observation $o_{t-T}, ..., o_t$ as input, where $T = 50$.

In order to train and conduct inference on the discriminator, we introduce the AMP observation denoted as s_t, which is comprised of joint positions, joint velocities, foot positions in base frame, base linear velocities, base angular velocities, and base height, resulting in a 67-dimensional vector. The input provided to the discriminator consists of the state transition (s_{t-1}, s_t).

A.2 Network Architecture

The teacher encoder is a 2-layer multi-layer perceptron (MLP) that takes the privileged information $x_t \in \mathbb{R}^{233}$ as input and outputs the latent vector $z_t \in \mathbb{R}^8$. The hidden layers have dimensions [256,128].

The base policy is a 3-layer multi-layer perceptron (MLP) that takes the current observation $o_t \in \mathbb{R}^{46}$ and the latent vector z_t as input and generates a 12-dimensional target joint angle output. The hidden layers have dimensions [512, 256, 128].

The student predictor begins by encoding each observation from recent steps into a 32-dimensional representation. Next, a one-dimensional convolutional neural network (1-D CNN) convolves these representations along the time dimension. The layer configurations, such as input channel number, output channel number, kernel size, and stride, are set to [32, 32, 8, 4], [32, 32, 5, 1], and [32, 32, 5, 1]. The flattened output from the CNN is then passed through a linear layer to predict $\hat{z}_t$.

The discriminator employs an MLP with hidden layers of size [1024, 512].

A.3 Learning Algorithm

We utilized Proximal Policy Optimization (PPO) as the reinforcement learning algorithm to train both the base policy and teacher encoder concurrently. The training process was composed of 50,000 iterations, with each iteration involving the collection of a batch of 131,520 state transitions. These transitions were evenly divided into 4 mini-batches for processing. To maintain a desired KL divergence of $KL^{desired} = 0.01$, we automatically tuned the learning rate using the adaptive LR scheme proposed by [35]. The PPO clip threshold was set to 0.2. For the generalized advantage estimation [36], we set the discount factor γ to 0.99 and the parameter λ to 0.95.

To optimize the objective defined in Eq (2), we trained the discriminator using supervised learning. We set the gradient penalty weight to $w^{\text{gp}} = 10$. The style reward weight is $w^s = 0.65$ and the task reward weight is $w^g = 0.35$.

The student encoder was trained with supervised learning, minimizing the mean squared error (MSE) loss between the latent vector z_t output by the teacher encoder and the predicted latent vector $\hat{z}_t$ output by the student encoder.

Throughout all training phases, we utilized the Adam optimizer with β values set to (0.9, 0.999), and ϵ set to $1e-8$.

A.4 Command Range

Table 1: Command Ranges for Different Terrains

	plane ground	stairs	discrete obstacles	uniform noise
lin vel cmd (m/s)	[-1.0,3.0]	[0,1.6]	[0,1.6]	[-1.0,2.5]
ang vel cmd (rad/s)	[-1.5,1.5]	[-1.0,1.0]	[-1.0,1.0]	[-1.5,1.5]

A.5 Domain Randomization

Table 2: Ranges of Randomization and Perturbations

environmental randomization	friction coefficient	[0.25,1.5]
	added mass	[-1.0,1.0]kg
	motor gain multiplier	[0.85,1.15]
perturbation	external torque	[-3.0,3.0]Nm
	linear velocity perturbation	[-1.0,1.0]m/s
	angular velocity perturbation	[-3.0,3.0]rad/s
sensor noise	joint position	[-0.03,0.03]rad
	joint velocity	[-1.5,1.5]rad/s
	base linear velocity	[-0.1,0.1]m/s
	base angular velocity	[-0.3,0.3]m/s
	gravity	[-0.49,0.49]m^2/s
	height measurement	[-0.01,0.01]m

B Experiment Results

B.1 Simulation Results

Table 3: Comparison of Success Rate and TTF

terrain types	controllers	success rate	TTF
uniform noise	complex rewards	0.9	0.98
	AMP	0.82	0.94
	ours	**0.92**	**1**
stairs	complex rewards	0.83	0.71
	AMP	0	0.12
	ours	**0.86**	**0.97**
discrete obstacles	complex rewards	0.54	0.86
	AMP	0.33	0.4
	ours	**0.92**	**0.98**

Table 4: Comparison of Energy Efficiency and Command Tracking Accuracy

terrain types		uniform noise			stairs			discrete obstacles		
controllers		complex rewards	AMP	ours	complex rewards	AMP	ours	complex rewards	AMP	ours
0.5m/s	acc(%)	**59.71**	53.73	57.45	38.80	\	**45.35**	\	\	**51.13**
	pow(W)	15.39	**13.75**	17.51	35.51	\	**20.60**	\	\	**28.87**
1.0m/s	acc(%)	**58.95**	45.32	57.34	24.86	\	**43.59**	\	\	**52.10**
	pow(W)	34.65	**19.48**	32.63	50.18	\	**36.11**	\	\	**50.93**
1.5m/s	acc(%)	55.56	33.25	**55.73**	10.09	\	**36.13**	\	\	**40.33**
	pow(W)	55.83	**41.99**	42.42	**43.53**	\	46.94	\	\	**62.51**
2.0m/s	acc(%)	**53.20**	21.64	48.60	\	\	**22.41**	\	\	**32.75**
	pow(W)	79.52	**49.84**	57.74	\	\	**65.80**	\	\	**69.43**
2.5m/s	acc(%)	**44.50**	9.34	42.55	\	\	\	\	\	\
	pow(W)	109.01	**9.33**	67.24	\	\	\	\	\	\

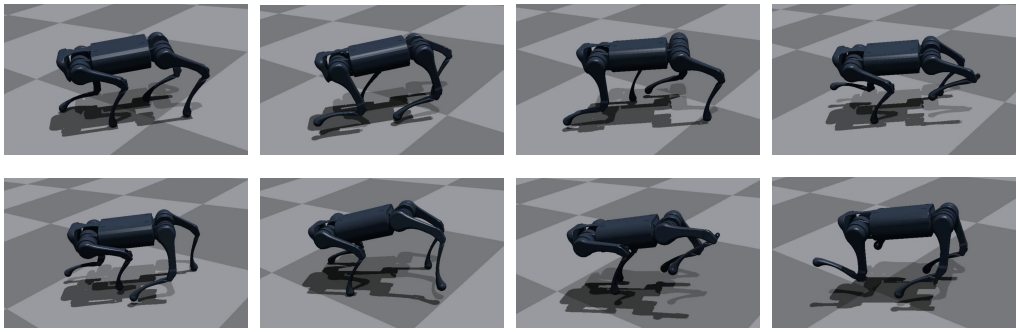

Figure 4: Snapshots of gaits captured at increasing speeds reveal the quadruped robot's transition from the 'trot' gait to the 'canter' gait, and eventually to the 'gallop' gait. This observation demonstrates the natural gait switching achieved by our learned controller.

B.2 Real World Results

Table 5: Comparison of Energy Efficiency

		Commanded Forward Velocity (m/s)	Complex Reward	AMP	Ours
Average Power (W)	w/ filter	0.5	24.39	15.62	**11.88**
		1.0	41.03	33.85	**33.13**
	w/o filter	0.5	25.88	20.66	**13.21**
		1.0	**48.53**	59.63	56.32

Table 6: Results of Real World Experiments

terrain type	controller	success rate	TTF	distance
13-cm step	complex reward	0.2	1	0.36
	AMP	0	1	0.2
	ours	**0.8**	**0.88**	**0.84**
grassland	complex reward	0.8	1	0.92
	AMP	0	0.1	0.1
	ours	**1**	**1**	**1**
slippery ground	complex reward	0	0.4	0.4
	AMP	0.2	0.6	0.68
	ours	**0.8**	**0.9**	**0.94**
staircase	complex reward	0	0.98	0.56
	AMP	0	0.68	0.1
	ours	**1**	**1**	**1**